https://doi.org/10.5194/egusphere-2026-1665
Preprint. Discussion started: 21 April 2026


# Methane emission quantification using UAV-based mass balance: Validation through controlled release experiments

Maria Tsivlidou[1], Jamie McQuilkin[1], Hugo Ricketts[1,2], Kieran Wood[3], Jonathan Helmore[4], David Lowry[5], and Grant Allen[1]

[1]Department of Earth and Environmental Sciences, University of Manchester, Oxford Road, Manchester M13 9PL, United Kingdom
[2]National Centre for Atmospheric Science, University of Manchester, Oxford Road, Manchester M13 9PL, United Kingdom
[3]School of Engineering, University of Manchester, Oxford Road, Manchester M13 9PL, United Kingdom
[4]National Physical Laboratory, Hampton Road, Teddington, Middlesex TW11 0LW, United Kingdom
[5]Department of Earth Sciences, Centre of Climate, Ocean and Atmosphere, Royal Holloway, University of London, Egham TW20 0EQ, United Kingdom

**Correspondence:** Maria Tsivlidou (maria.tsivlidou@manchester.ac.uk) and Grant Allen (grant.allen@manchester.ac.uk)

**Abstract.** Uncrewed aerial vehicles (UAVs) offer flexible and cost-effective access to monitoring methane sources that can be otherwise difficult to sample, but confidence in UAV-derived fluxes requires robust validation and uncertainty characterisation. Here, we evaluate a variant UAV-based mass-balance method using single-blind controlled-release experiments at two UK sites: An aerodrome in Bedford and the Centre for Dairy Research (CEDAR), Reading. Controlled methane releases ranged from 0.021 to 2.16 $\mathrm{kg\ h^{-1}}$ in Bedford and 8.3 to 40.6 $\mathrm{kg\ h^{-1}}$ in CEDAR, including point and extended source configurations. Methane concentrations were measured in situ using an ABB GLA133-GPC analyser mounted on a hexacopter UAV equipped with a 2D sonic anemometer, and fluxes were derived from downwind horizontal transects.

Two validation approaches are considered: (i) using all individual flights to capture operational variability, and (ii) grouping flights by release rate to assess underlying method performance. Overall, fluxes calculated using the method show good correlation but substantial scatter at the individual flight level (CEDAR: slope = 1.01, $r$ = 0.84, RMSE = 38.8%; Bedford: slope = 0.71, $r$ = 0.85, RMSE = 46.2%) and substantially improved agreement when averaged by release rate (CEDAR: slope = 1.01, $r$ = 0.94, RMSE = 19.9%; Bedford: slope = 0.68, $r$ = 0.99, RMSE = 38.4%). This demonstrates that averaging reduces random variability while preserving systematic bias.

A method variant, which accounts for incomplete near-surface sampling by extrapolating the lowest available measurements and incorporating the associated uncertainty, substantially improves consistency, increasing the fraction of cases (46% to 72%) in which the known release rate falls within the one-standard-deviation uncertainty of the calculated release rate. We find that mean wind speed is the dominant environmental factor influencing the quality of agreement, with higher wind speeds associated with reduced bias (above 2.2 $\mathrm{m\ s^{-1}}$, bias $\leq$ 50%), likely due to reduced turbulence under such conditions. Wind direction variability alone shows little direct influence on flux precision; instead, a wide lateral extent of the measurement plane is noted to be critical for minimising plume sampling loss under changing wind conditions. Lower emission rates exhibit greater relative bias due to increased sensitivity to smaller signal-to-noise (due to both wind variability and lower plume concentration enhancements relative to natural background variability).

https://doi.org/10.5194/egusphere-2026-1665
Preprint. Discussion started: 21 April 2026


The improved performance after averaging is consistent with previous studies indicating that multiple flights per release rate (e.g. $n \geq 3$) enhance representativeness by reducing the influence of environmental variability. These results demonstrate that UAV-based mass-balance methods can provide methane flux estimates accurate to within 20%, for fluxes greater than 10 $\mathrm{kg\ h^{-1}}$, under controlled conditions, but may suffer from systematic (but accountable) under-bias due to incomplete sampling. We also offer insights on methodological and environmental requirements to deliver robust measurements.

## 1 Introduction

Methane ($CH_4$) is the second-most important anthropogenic greenhouse gas after carbon dioxide ($CO_2$) in terms of radiative forcing (Etminan et al., 2016), with a 20-year global warming potential more than 80 times higher than $CO_2$ (IPCC, 2023). Responsible for nearly 30% of observed global warming (Shan et al., 2025), atmospheric $CH_4$ concentrations have increased 2.6-fold since 1750, reaching 1942 $\pm 2$ ppb in 2024 (WMO, 2025). Approximately two-thirds of emissions are anthropogenic in 2020, primarily from agriculture (41% of total emissions, ∼80% from livestock and manure and ∼20% from rice cultivation), fossil fuels (33%), and landfill and waste management (19%) (Saunois et al., 2025). Global $CH_4$ emissions reached 608 $\mathrm{Tg\ yr^{-1}}$ in 2020—about 12% above the 2000-2010 average—highlighting ongoing increases in anthropogenic sources (Saunois et al., 2025).

Due to its relatively short atmospheric lifetime (∼9 years; Prather et al., 2012), $CH_4$ is a key target for near-term climate mitigation (Shindell et al., 2012; UNEP, 2021). In support of this, 159 countries have joined the Global Methane Pledge, committing to a 30% reduction in anthropogenic emissions by 2030. Effective mitigation offers co-benefits including improved public health and agricultural productivity (Global Methane Pledge, 2023).

Despite progress, large uncertainties persist in the global $CH_4$ budget. Top-down atmospheric inversions estimate 575 $\mathrm{Tg\ yr^{-1}}$ for 2010–2019, whereas bottom-up inventories suggest 669 $\mathrm{Tg\ yr^{-1}}$ (Saunois et al., 2025). Although alignment between methods has improved, significant discrepancies remain, limiting the reliability of emission inventories and hindering effective mitigation monitoring. For the decadal $CH_4$ budget, sectoral uncertainties range from 20% to 35% for agriculture, waste, and fossil fuels, ∼50% for biomass burning and wetlands, and up to 100% for other natural sources such as inland waters and geological seepage (Tibrewal et al., 2024; Saunois et al., 2025).

Independent observational methods are essential to constrain these uncertainties. Satellites (e.g., Pandey et al., 2021; Schuit et al., 2023) provide daily global coverage but are limited by coarse spatial resolution and detection thresholds (∼100 $\mathrm{kg\ h^{-1}}$; Cooper et al., 2022; Jacob et al., 2022). Airborne campaigns (e.g., Pitt et al., 2019) can target specific sources, but they are costly and typically operate at high speeds and altitudes, causing the collected data to reflect averages across large horizontal scales, which may limit the resolution of fine-scale spatial patterns (Li et al., 2025).

Uncrewed aerial vehicles (UAVs) offer a flexible, cost-effective, and scalable approach for localised $CH_4$ monitoring. Equipped with lightweight sensors, they can provide high-resolution horizontal and vertical measurements that complement satellite and aircraft data, making them well suited for leak detection, source attribution, and facility-scale quantification (Yang

https://doi.org/10.5194/egusphere-2026-1665
Preprint. Discussion started: 21 April 2026


et al., 2018; Shaw et al., 2021; Souza et al., 2024). Advances in sensor technology have extended UAV capabilities to remote or hazardous environments, including rugged terrain, volcanic areas, and natural gas infrastructure (Li et al., 2025).

UAV-based $CH_4$ emission quantification commonly relies on mass balance approaches that integrate downwind $CH_4$ concentration enhancements (relative to the ambient background concentrations) with wind fields (Allen et al., 2018, 2019; Shaw et al., 2021). These approaches provide a practical and flexible framework for facility-scale emission estimation, but their quantitative interpretation depends on how well the measurements represent the spatial structure of the plume and the prevailing atmospheric conditions (Fosco et al., 2024; Yong et al., 2024). More broadly, accurate methane quantification requires not only robust measurement techniques but also representative and clearly reported uncertainties to establish confidence in derived emission estimates. Previous work has shown that method performance depends on atmospheric variability, experimental design, and analysis choices, underscoring the need for validation against known reference emissions using controlled or blind release experiments (e.g., Morales et al., 2022; Liu et al., 2023). Despite increasing application of UAV-based methods, the methane measurement community currently lacks a standardised framework for validating quantification approaches and reporting uncertainties, which limits comparability between studies and confidence in reported emissions (Riddick et al., 2023; Connor et al., 2024).

Controlled-release experiments, in which emission rates and locations are independently known, provide a critical means of evaluating uncertainties and validating UAV-based methane quantification methods (Feitz et al., 2018; Shah et al., 2020a). However, controlled-release evaluations of UAV-based mass balance approaches remain relatively limited, and systematic characterisation of uncertainties across operating conditions is still lacking (e.g. Allen et al., 2018; Morales et al., 2022; McManemin et al., 2025; Scheutz et al., 2025). Reducing these uncertainties is critical for improving emission inventories and supporting effective mitigation.

Here, we conducted controlled-release experiments at two UK test sites over two weeks in May 2024 and September 2025, using a UAV equipped with a high-precision $CH_4$ sensor and a sonic anemometer to perform downwind measurements. A mass balance method was applied to estimate emissions, enabling evaluation of the system's performance near its detection limit and improving the characterisation of flux uncertainties for facility-scale monitoring.

In this paper, we present the experimental setup, UAV flight strategy, and analytical framework, and assess the performance of mass balance $CH_4$ quantification under controlled, yet meteorologically realistic, conditions.

## 2 Data and methods

### 2.1 Instrumentation

#### 2.1.1 UAV platform and payload

In this study, a DJI M600 Pro hexacopter (9.5 kg with six batteries; Fig. 1) was used. It provides up to 32 min hover time without payload or 16 min with a 6 kg payload (DJI, 2025). As a rotary-wing UAV, the M600 Pro flies slower than fixed-wing

https://doi.org/10.5194/egusphere-2026-1665
Preprint. Discussion started: 21 April 2026


UAVs, allowing denser sampling and greater manoeuvrability—beneficial for detailed surveys in complex sites such as landfills (Allen et al., 2019; Fosco et al., 2024; Yong et al., 2024).

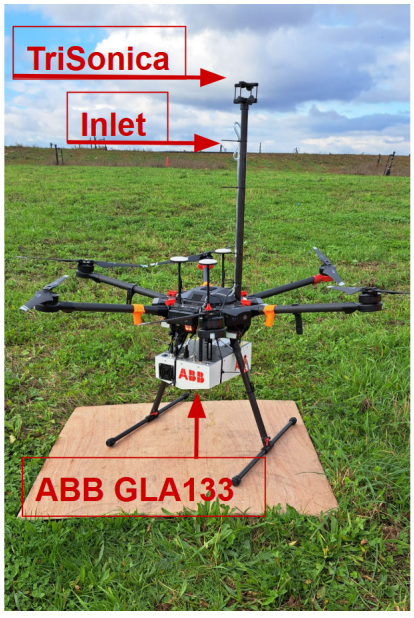


**Figure 1.** UAV platform and payload. The DJI M600 Pro hexacopter is equipped with an ABB GLA133-GPC OA-ICOS infrared spectrometer, a gas sampling inlet, and a TriSonica Mini anemometer. Arrows indicate the positions of each component used for atmospheric measurements.

The payload was an ABB GLA133-GPC greenhouse gas analyser (3 kg; Fig. 1), mounted beneath the UAV with a 0.3 m inlet positioned above the rotor plane. This Off-Axis Integrated Cavity Output Spectroscopy (OA-ICOS) instrument measured $CH_4$ at 5 Hz, with calibrated $1\sigma$ precision of 0.9 ppb, and transmitted real-time data wirelessly during flight to support pilot oversight when required. Wind was measured on board using a LI-550 TriSonica™ Mini Wind and Weather Sensor (Fig. 1), capable of measuring wind speed from 0–50 $\mathrm{m\,s^{-1}}$ with 0.01 $\mathrm{m\,s^{-1}}$ resolution and accuracy of $\pm 0.2$ $\mathrm{m\,s^{-1}}$ for speeds between 0 and 10 $\mathrm{m\,s^{-1}}$, $\pm 2\%$ for speeds between 11 and 30 $\mathrm{m\,s^{-1}}$, and $\pm 4\%$ for speeds between 31 and 50 $\mathrm{m\,s^{-1}}$. The sampling frequency of the anemometer was $5\mathrm{Hz}$. Wind direction measurements for the horizontal wind components (u and v) were recorded over a range of 0–359°with a resolution of 1.0°and an accuracy of $\pm 1.0°$. The vertical wind direction component (w) was measured within $\pm 15°$from the horizontal plane of the instrument, with an accuracy of $\pm 2°$. To avoid interaction with the rotor air flow, the anemometer was mounted on a 65 cm mast above the rotor plane.

For navigation and flight planning, the ABB GLA133-GPC analyser integrated hardware and software to synchronise all payloads, recording flight and sensor data in unified files. This ensured accurate geolocation of gas concentration and wind measurements. Automated flight paths were pre-planned using UgCS software (SPH Engineering, 2025), providing repeatable surveys with constant speed, altitude, and coverage, and reducing operator bias (which can translate into emissions bias as described in Shah et al. (2020a, b)). Flights were conducted at 3–4 $\mathrm{m\,s^{-1}}$; below 5 $\mathrm{m\,s^{-1}}$ the UAV horizontal tilt angle is

https://doi.org/10.5194/egusphere-2026-1665
Preprint. Discussion started: 21 April 2026


small, negating the need for a challenging tilt correction in 2D wind measurements. Using the autopilot system maintained smooth steady flight with no rapid motions during the transects, which reduced artifacts (compared to work reported in Yong et al. (2024)). In addition, its use avoided over-sampling bias within plumes, improving $CH_4$ flux accuracy in terms of the sampling concepts and assumptions implicit to the mass balance method (see Sect. 2.2).

#### 2.1.2 Ground-based meteorological instrumentation

To assess the performance of the UAV-mounted Trisonica anemometer, wind fields were also measured using four Gill MetPak Pro instruments mounted on a ground mast at heights of 3, 6, 9, and 12 m above ground level, recording 1-minute average wind speed and direction. These mast-based measurements were used exclusively for comparison with winds measured by the UAV-mounted anemometer and were not used in the mass-balance flux calculations, which rely solely on UAV-mounted anemometer wind data. A comparison showed reasonable temporal agreement between the mast-based and UAV-mounted anemometer wind direction, with small remaining differences in wind speed attributed to the height of the mast versus UAV flight altitude, and the 1-minute sampling of the mast. This provides confidence (and preference) in the use of the on-board wind measurements for emission quantification.

### 2.2 UAV-based mass balance flux method

To calculate $CH_4$ emissions, we applied a mass balance approach (Allen et al., 2014, 2018; Shaw et al., 2021), widely used across environments including landfills (Allen et al., 2019; Yong et al., 2024), urban areas (Pitt et al., 2019; Tong et al., 2023), and wetlands (Barker et al., 2022). The method estimates flux by measuring concentration differences inside and outside a defined downwind plane perpendicular to the prevailing wind.

For each survey, flight paths were designed with respect to wind direction to ensure full plume capture. The UAV was flown downwind of the release point and executed a vertical "ladder" pattern of stacked horizontal parallel transects at multiple altitudes, enabling assessment of emissions across plume heights. The distance between the transects is predetermined and kept constant.

The $CH_4$ emission rate $F$ ($\mathrm{g\ s^{-1}}$) is given by:

$$F = \int_{x_1}^{x_2} \int_{z_1}^{z_2} \left([\mathrm{CH_4}] - [\mathrm{CH_4}]_{\mathrm{background}}\right) U_{\perp}\, dx\, dz \tag{1}$$

Where $U_{\perp}$ is the normal component of the wind speed with respect to the measurement plane ($\mathrm{m\ s^{-1}}$), and $[CH_4]$ and $[CH_4]_{background}$ are the $CH_4$ concentrations ($\mathrm{g\ m^{-3}}$) within the plume and the ambient background, respectively. In this study, the $[CH_4]_{background}$ was derived from measurements collected outside of the plume during each downwind survey, rather than from separate upwind flights. Based on field experience, ambient $CH_4$ can vary on timescales of roughly an hour, so a flight-specific background provides a more accurate representation of the conditions at the time of measurement. Further information about the $[CH_4]_{background}$ can be found in Appendix A. Equation 1 is integrated over the horizontal ($x_1$ to $x_2$) and vertical ($z_1$ to $z_2$) measurement ranges.

https://doi.org/10.5194/egusphere-2026-1665
Preprint. Discussion started: 21 April 2026


To account for unsampled locations within the survey area (and flux plane), we applied kriging, a geostatistical interpolation technique that estimates values at unmeasured points based on spatial correlations in the data (Myers, 1991). This method assumes that nearby observations are more similar than those farther apart, allowing for the interpolation of $CH_4$ concentrations and wind velocities onto a continuous grid. By using kriging to map the full extent of the plume, we minimize underestimation of the flux and improve the spatial resolution of our mass balance calculations (Allen et al., 2015; Mays et al., 2009).

A single UAV flight survey provides a snapshot of the plume and enables the estimation of a single flux value, assuming that the emission source strength and the plume morphology remain relatively constant during the flight (Yong et al., 2024). While the method assumes that the plume and emission source are stable during this time, fluctuations in $CH_4$ concentrations and wind conditions may introduce uncertainty in the flux estimate. Any mass balance method using an in situ sensor on a moving platform cannot account (or reliably estimate) for dynamic sources that may vary over the length of any survey. Thus, in previous studies, a static source is implicitly assumed. This is also the case here, and the controlled releases were static over the course of single surveys for validation.

Flux uncertainty was quantified by propagating the relative uncertainties of background concentration and perpendicular wind speed, following Allen et al. (2018):

$$F_{\text{uncertainty}} = \sqrt{\left(\frac{\sigma_{\text{background}}}{\mu_{\text{background}}}\right)^2 + \left(\frac{\sigma_{\text{wind}}}{\mu_{\text{wind}}}\right)^2} \tag{2}$$

where $\sigma$ and $\mu$ are the standard deviation and the mean value of each component respectively. This approach accounts for variability in both key input parameters to the flux equation, ensuring a more robust (and fully traceable) estimate of flux uncertainty, which is directly derived from measurable sources of environmental variability.

### 2.2.1 Adaptation of the UAV-Based Mass Balance Flux Method

Despite their strong applicability for methane emission monitoring and their flexibility in accessing hazardous or otherwise unapproachable sources (Li et al., 2025), UAV-based measurements have various important limitations. A common limitation of UAV-based flux estimates is the inability to sample very close to the ground due to safety constraints or obstacles. More discussion on this topic follows in Sect. 3. Since methane concentrations are typically highest near the surface, this can lead to systematic underestimation of fluxes. To assess this, fluxes in the near-ground layer were estimated by extrapolating $CH_4$ concentrations from the lowest sampled heights (Fig. 2).

The extrapolated contribution was not added to the flux estimate itself, but rather incorporated into the positive uncertainty bound (as it represents an expected under-bias), resulting in an asymmetric error range. Flux uncertainty was calculated as in Equation 2, with the extrapolated near-ground flux term $F_{extrapolated}$ added only to the upper error bar:

$$\sigma_F^- = F_{\text{uncertainty}} \; and \; \sigma_F^+ = F_{\text{uncertainty}} + F_{\text{extrapolated}} \tag{3}$$

https://doi.org/10.5194/egusphere-2026-1665
Preprint. Discussion started: 21 April 2026


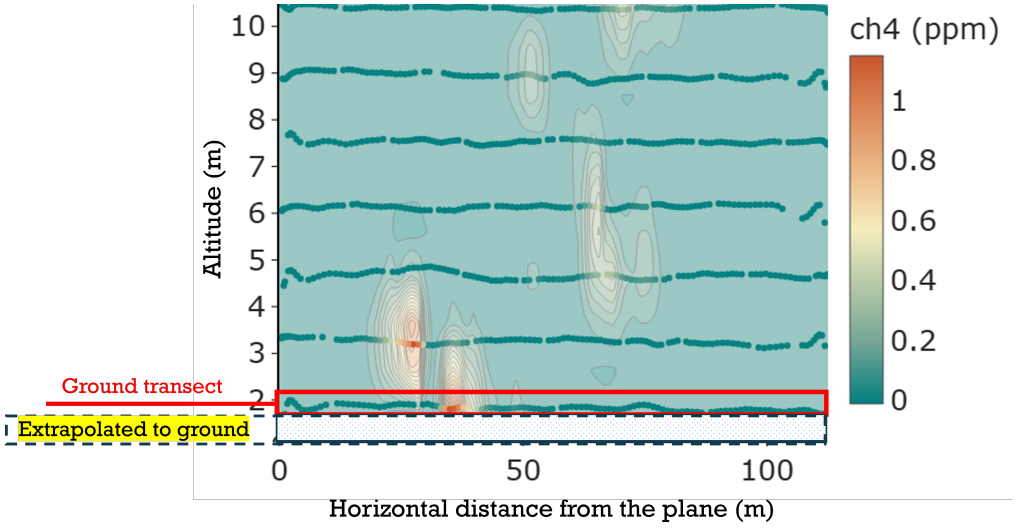


**Figure 2.** Example flight showing the lower transect (∼2m) used to extrapolate near-ground flux. The resulting contribution is included in the positive flux uncertainty.

This approach retains the central flux estimate strictly based on measured concentrations, while accounting for the potential influence of unsampled near-surface layers within the positive uncertainty range. Because near-surface concentrations are not directly observed, their estimation relies on extrapolation assumptions that may not hold uniformly across stability regimes or surface conditions. Incorporating this contribution as an uncertainty term avoids introducing method-dependent bias or artificial enhancement of emissions, preserves traceability to the measurements, and ensures methodological consistency across flights with varying sampling constraints. This conservative treatment improves the robustness and transparency of the mass balance framework.

## 2.3 Controlled-release experiments

Controlled methane release experiments were conducted by the National Physical Laboratory (NPL) at two UK test sites: Bedford Aerodrome (13–17 March 2024) and the Centre for Dairy Research (CEDAR), University of Reading (8–10 September 2025) (Fig. 3a and b). At Bedford Aerodrome, controlled releases were created using NPL's miniature Controlled Release Facility (mini-CRF), while at CEDAR the CFR, a higher emission rate system, was used. Both systems are mobile gas release setups designed to produce accurately quantified methane fluxes under field conditions, operating on the same principle as arrays of mass flow controllers (Brooks Instruments) calibrated volumetrically for methane using Mesa Labs ML800 and ML1020 piston-type flow meters. The release systems were calibrated using high-accuracy reference flow meters traceable to national standards. Volumetric flow rates were standardised to 273.15 K and 1013.25 hPa. The volumetric emission rates were converted to mass emission rates at these conditions (i.e. using a molar volume of 22.414 L $\mathrm{mol}^{-1}$. Each site was instrumented with a ground-based meteorological mast (see Sect. 2.1.2).

https://doi.org/10.5194/egusphere-2026-1665
Preprint. Discussion started: 21 April 2026


For both experiments, the methane release rates were kept blind to analysts until completion of data processing, ensuring an unbiased performance assessment. UAV-based plume sampling and flux estimation were conducted using the mass balance method described in Sect. 2.2. This approach enabled evaluation of system performance near the lower detection limit and characterisation of flux uncertainties under realistic operational conditions.

Further details on the experimental sites and the prevailing meteorological conditions during the campaigns are provided in the following subsections. An overview of the experiments conducted at each site is summarised in Table 1.

### 2.3.1 Bedford Aerodrome

The Bedford Aerodrome site (a former runway; Fig. 3a and c) was used to test point and elevated sources (Table 1). Release rates ranged from 0.021 to 2.16 $\mathrm{kg\,h^{-1}}$ and were emitted from ground level, 1 m, and 3 m sources to represent realistic scenarios such as manure piles and equipment leaks. Also, this flux range is consistent with methane emission rates reported for a range of oil- and gas-related infrastructure, including natural gas distribution systems (Lamb et al., 2015) and lower-emission production facilities (Vollrath et al., 2024). No heat exchangers were used at this site (to equilibrate cold gas leaving supply cylinders), but the length of hose between supply cylinders and outlets is considered to be sufficient to reach ambient temperature on release.

In addition to the UAV-based measurements, the Bedford campaign included multiple ground-based teams conducting independent methane surveys. Some of the ground-based measurements from this experiment are reported in Tettenborn et al. (2025), which evaluates emission estimation methodologies using controlled releases up to 2.8 $\mathrm{kg\,h^{-1}}$.

For the UAV-based measurements presented here, the first two days (13-14 May 2024) were dedicated to setting up and test flights on the site. The flights used for quantification were conducted on 15 and 16 May 2024. Weather was generally stable, with light to moderate winds: 3.07–4.63 $\mathrm{m\,s^{-1}}$ on 15 May 2024, 2.32–3.91 $\mathrm{m\,s^{-1}}$ on 16 May 2024 (range of average on-board wind speed during flights).

In total, 24 flights were carried out, for seven different release rates and three different types of emission sources (Table 1).

https://doi.org/10.5194/egusphere-2026-1665
Preprint. Discussion started: 21 April 2026


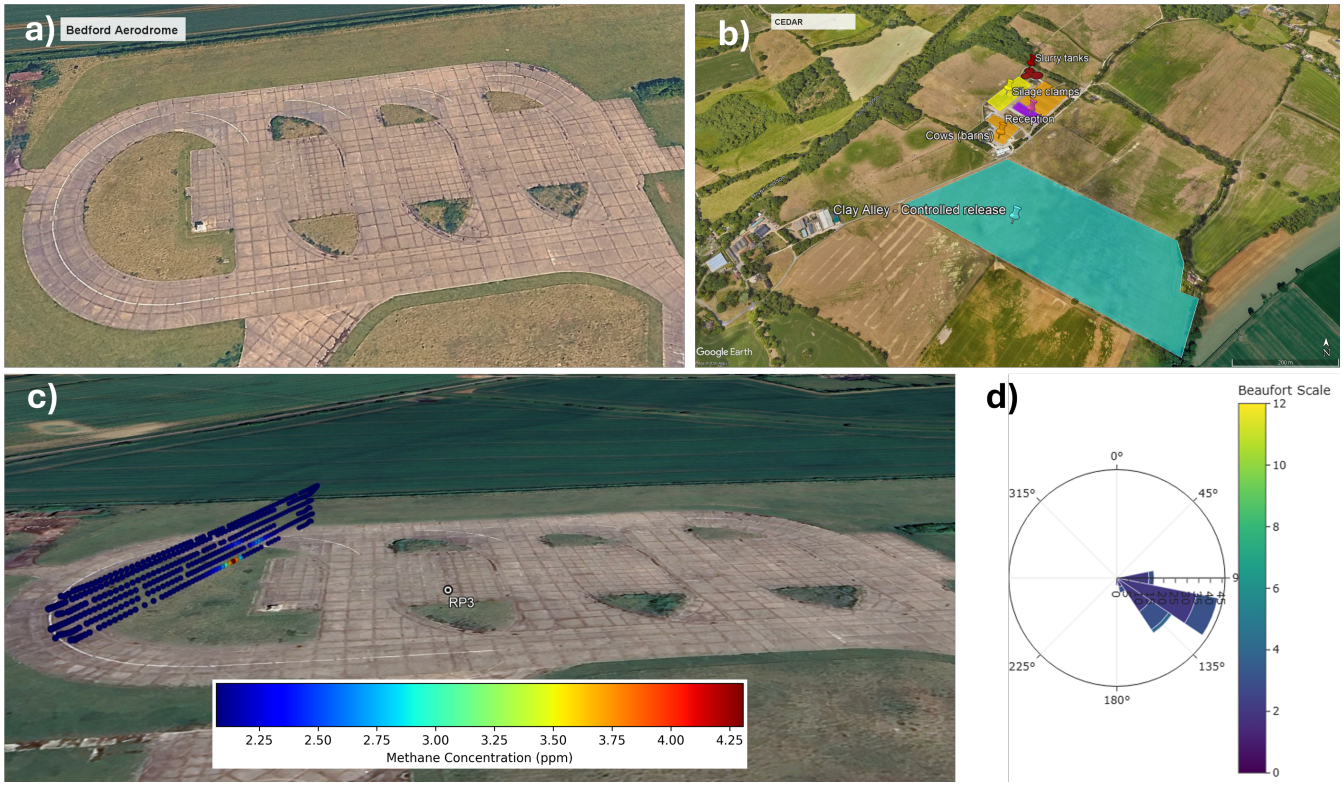


**Figure 3.** (a) Bedford Aerodrome showing methane release points (RP1–RP6), with one active at a time. (b) Aerial view of the CEDAR site. (c) Example UAV flight path downwind of a release point, illustrating the vertical "ladder" transect pattern used for $CH_4$ measurements. (d) Wind rose corresponding to the same flight. Imagery: © Landsat / Copernicus, Map data: © 2026 Google.

### 2.3.2 Centre for Dairy Research, University of Reading

At the CEDAR site (Fig. 3b), experiments were designed to mimic distributed landfill-type emissions using a linear ground-level source approximately 60 m in length. The source was orientated nominally perpendicular to wind direction before conducting each controlled release test. Release rates ranged from 8.3 to 40.6 $\mathrm{kg\,h^{-1}}$, substantially higher than those used at Bedford, thereby extending the validation across a wider emission range representative of landfill-scale sources (e.g. Mønster et al. (2019)). At the CEDAR site, the release system incorporated inline heat exchangers to raise the emitted gas temperature to near-ambient conditions prior to release. Direct measurement of the outflow gas temperature was not performed; however, the inclusion of heat exchangers ensured that the released methane was at or close to ambient temperature at the point of emission.

Four independent UAV teams collected data during the campaign. Here, we report only the flights and measurements conducted by our team.

The experiment was conducted under generally stable weather, with winds ranging from moderate to stronger speeds (5.80–7.04 $\mathrm{m\,s^{-1}}$ on 08 September, 4.77–6.70 $\mathrm{m\,s^{-1}}$ on 09 September and 4.34-5.03 $\mathrm{m\,s^{-1}}$ on 10 September). During these

https://doi.org/10.5194/egusphere-2026-1665
Preprint. Discussion started: 21 April 2026


**Table 1.** Overview of controlled release experiment sites.

| | Bedford | CEDAR |
|---|---|---|
| $CH_4$ release rate | 0.021 to 2.16 kg $h^{-1}$ | 8.3 to 40.6 kg $h^{-1}$ |
| Source characteristics | Ring source at 1 m (RP2), linear vertical source from ground to 3 m (RP3), and point source at 1 m (RP4) | Linear source of approx. 60 m length at ground level |
| Heat exchangers used | No | Yes (Gas expected near ambient temperature) |
| Wind conditions | 15/05/2024: 4.07 m $s^{-1}$<br>16/05/2024: 2.19 m $s^{-1}$ | 08/09/2025: 6.35 m $s^{-1}$<br>09/09/2025: 5.67 m $s^{-1}$<br>10/09/2025: 4.57 m $s^{-1}$ |
| Number of flights | 24[α] | 14 |
| Take off and landing | Manually-piloted | Manually-piloted |
| Flight control | Manually-piloted | Automated way point flying |
| Distance from source | 56-110 m | 87-187 m |

[α] RP2: 3 flights; RP3: 13 flights; RP4: 8 flights.

days, the wind was from the south, so the controlled release plume was advected toward the UAV measurement setup, while the slurry tanks and barn were located downwind of the sampling area. Therefore, emissions from these structures did not influence the UAV-based $CH_4$ estimates.

A total of 14 flights were conducted, for four different release rates and one source type (Table 1).

## 3 Results and discussion

Figure 4 shows the comparison between UAV-estimated fluxes and controlled release fluxes for Bedford and CEDAR, considering both individual flights (a, b) and release-rate-averaged data (c, d). The error bars in the estimated fluxes are a combination of the uncertainty of the flux and the extrapolated flux above the ground (Sect. 2.2.1). This is discussed further later in this Section. The ordinary least-square-fit line is also included, along with the 1:1 line (y=x) which would indicate perfect agreement to support data interpretation. Generally, data points below (resp. above) this line are related to an underestimation (resp. overestimation) in the flux estimation. To quantify the performance of the comparison, the bias (in kg $h^{-1}$ and %) is calculated and included in Table 2.

Using all individual flights (Fig. 4a, b), the comparison shows good correlation but substantial scatter at both sites. At Bedford, the ordinary least squares (OLS) fit yields a slope of 0.71 with Pearson r = 0.85, indicating a systematic underestimation and moderate dispersion (RMSE = 46.2%, bias = -38.5%). At CEDAR, the OLS slope is close to unity (1.011) with r = 0.84, suggesting good proportional agreement, although variability remains (RMSE = 38.8%), with a small positive bias (∼2%).

https://doi.org/10.5194/egusphere-2026-1665
Preprint. Discussion started: 21 April 2026


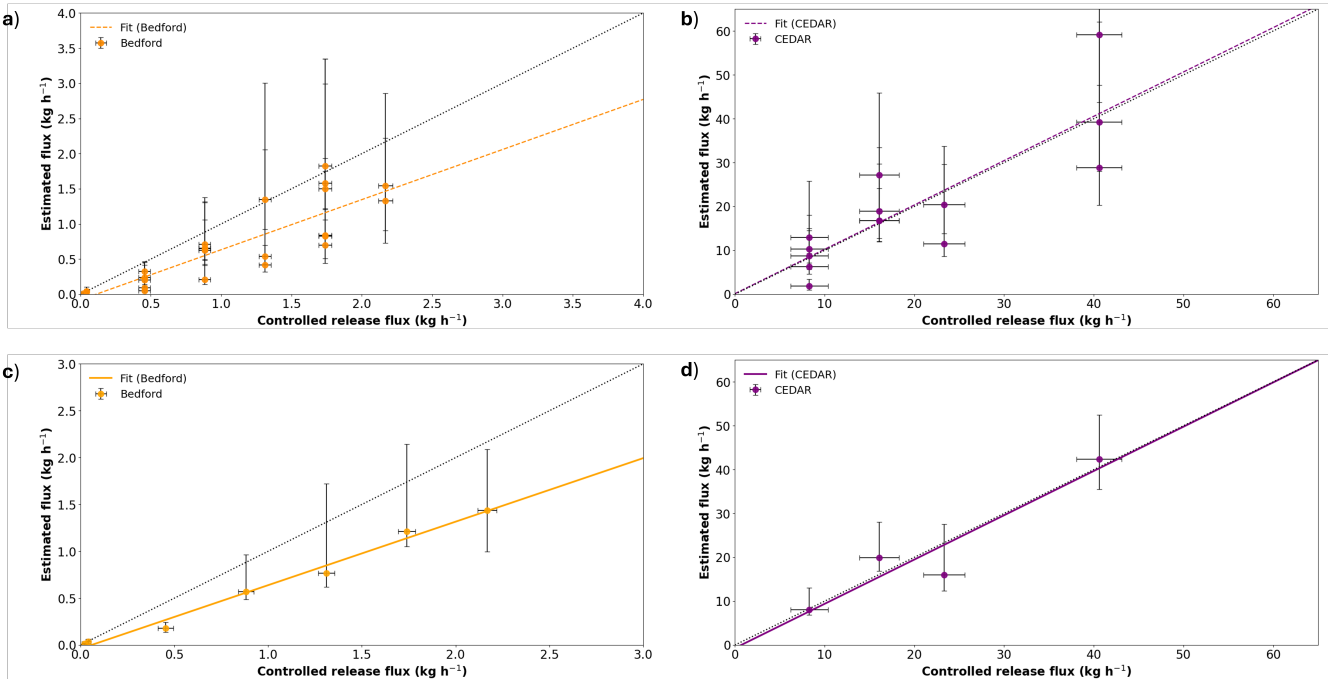


**Figure 4.** Comparison of $CH_4$ fluxes estimated from UAV-based measurements with known controlled release rates for CEDAR and Bedford, considering individual flights (a, b) and release-rate-averaged data (c, d). In both cases, vertical error bars indicate UAV-based flux uncertainties and horizontal error bars represent release uncertainties. Least-squares regression lines are shown for each panel, while the black dashed line indicates the 1:1 relationship (y = x). Axes limits differ between panels to match the range of observed release rates.

When grouping flights by release rate and averaging multiple survey flux measurements (Fig. 4c, d), the agreement improves substantially. At Bedford, the correlation increases to r = 0.994 with a similar slope (0.68), and RMSE decreases to 38.4%, while bias remains comparable (-36.5%). At CEDAR, the averaged results show near-perfect agreement (slope = 1.01, r = 0.94) and very low bias (-1.63%) and RMSE (19.9%). It is also note worthy that all of the controlled release rates are captured by the $1\sigma$ uncertainty ranges of the release-rate-averaged UAV-based estimated fluxes. The improvement observed after averaging is consistent with previous studies indicating that a minimum number of repeated flights per release rate (e.g. $n \geq 3$ Scheutz et al., 2025) enhances representativeness. In this study, the reduced scatter and increased correlation in the averaged results suggest that individual flights are influenced by variability in environmental conditions, whereas aggregating multiple flights provides a more robust estimate of the true flux.

The better agreement for CEDAR data could be due to several reasons related to the design of the experiment, as well as the fact that CEDAR release rates were much larger than those at Bedford (and therefore experience a better environmental signal-to-noise in the terms of the parameters implicit to the mass balance flux equation, such as the relative importance of natural background variability). A specific design factor is expected to be the use of automated waypoint flying at CEDAR, compared with manually piloted flights in Bedford. The automated waypoint flying enabled repeatable and objective surveying

https://doi.org/10.5194/egusphere-2026-1665
Preprint. Discussion started: 21 April 2026


**Table 2.** Mean bias (kg $h^{-1}$, %) by known rate, including site, source type and number of flights.

| Site | Known rate | Source type | N (flights) | Mean bias $^{\alpha}$ (kg $h^{-1}$) | Mean bias $^{\beta}$ (%) |
|---|---|---|---|---|---|
| Bedford | 0.021 ± 0.012 | 1 m, Ring | 1 | -0.0077 | -36.4 |
| | 0.042 ± 0.013 | 1 m, Ring | 2 | -0.0073 | -17.3 |
| | 0.45 ± 0.041 | Ground - 3 m, Linear vertical | 5 | -0.27 | -60.5 |
| | 0.88 ± 0.041 | Ground - 3 m, Linear vertical | 5 | -0.31 | -35.5 |
| | 1.31 ± 0.043 | 1 m, Point | 3 | -0.54 | -41.5 |
| | 1.73 ± 0.045 | Ground - 3 m, Linear vertical | 6 | -0.52 | -30.4 |
| | 2.16 ± 0.049 | Ground - 3 m, Linear vertical | 2 | -0.73 | -33.7 |
| CEDAR | 8.3 ± 2.1 | Ground, Linear (60 m length) | 5 | -0.26 | -3.2 |
| | 16.1 ± 2.2 | Ground, Linear (60 m length) | 4 | 3.81 | 23.7 |
| | 23.3 ± 2.3 | Ground, Linear (60 m length) | 2 | -7.33 | -31.5 |
| | 40.6 ± 2.5 | Ground, Linear (60 m length) | 3 | 1.81 | 4.5 |

$^{\alpha}$ Estimated flux minus controlled release flux.
$^{\beta}$ 100 × (estimated flux - controlled release flux) / controlled release flux.

by maintaining constant speed, altitude, and coverage across surveys, reducing variability and potential bias introduced by manual control (Shah et al., 2020a, b). Automated flight paths ensured optimized area coverage with minimal overlap or gaps, improving data quality and comparability. The UAV speed was also set lower than in the manual flights, resulting in more dense sampling of the plume with higher spatial resolution in the measurements. In addition, the lower UAV speed resulted in higher measurement duration, meaning integrating more data and therefore a decrease in measurement error (Liu et al., 2023). Another contributing factor may be the use of heat exchangers in the CEDAR site, which resulted in methane temperatures close to ambient conditions. Although colder-than-ambient emission at Bedford was not expected (as discussed in Sect. 2.3.1), it cannot be ruled out. Improved plume mixing and capture may also be influenced by the distance from the emission source. At the Bedford site, measurements were conducted at distances of 56–110 m from the source (Table 1), whereas at CEDAR the measurement distances were larger, ranging from 87–187 m. In addition, the controlled release rates at CEDAR were substantially higher than those at Bedford. As a result, the lower release rates at Bedford were more sensitive to atmospheric turbulence and wind variability, particularly under the lower wind speed conditions observed during that experiment. Furthermore, at low emission rates, small absolute differences between estimated and true fluxes can result in disproportionately large relative (percentage) biases. This effect may therefore contribute to the higher apparent bias observed at lower release rates.

To investigate further any potential relationship between the bias and the release rate, Fig. 5 shows the bias in % for all the flights and for different bins of controlled released rates of 0-0.1, 0.1-1, 1-10 and larger than 10. Across all flights, the average bias is approximately -25% compared to the controlled released rates. Focusing on the different bins in Fig. 5, we see that there

https://doi.org/10.5194/egusphere-2026-1665
Preprint. Discussion started: 21 April 2026


is no strong fundamental dependence on the release rate or the source type. We can conclude from this that the quantification method is capable of capturing both small localised emissions close to the ground (ring or point emissions located at 1 m), larger extended ground-level emissions (60 m linear sources) and vertically distributed emissions (linear vertical sources from ground to 3 m). Indeed, the lowest bias is observed for higher release rates (Table 2), as larger concentration enhancements relative to background variability result in a higher signal-to-noise ratio and reduced sensitivity to turbulence and wind variability. This leads to a more coherent plume structure and more robust flux estimation.

Previous studies have also conducted controlled release experiments to validate UAV-based mass balance methods. Among all 45 quantifications of the TADI campaigns conducted by Bonne et al. (2024), the relative errors of all quantifications span -69% to +149% (relative error of -41% in terms of total emitted mass during all campaigns). A logarithmic interpolation was performed to interpolate the values of q(z) below the lowest transect, considering zero flux at the ground level. Morales et al. (2022) conducted controlled-release tests and reported normalized mean absolute percentage errors of 54–71%, primarily due to systematic underestimation when the full vertical extent of the plume was not captured at greater downwind distances. Similarly, Scheutz et al. (2025) validated a UAV-based method that simultaneously measured $CH_4$ concentrations and wind vectors, achieving emission quantification errors ranging from +33% to –35% in controlled releases. The results in our work (-36.5% at Bedford, and -1% at CEDAR) are consistent with, and in the case of CEDAR improve upon, previously reported UAV-based validation results which supports the validity and robustness of the mass balance method for the quantification of greenhouse gas emissions with careful sampling design and high-precision UAV-mounted sensors.

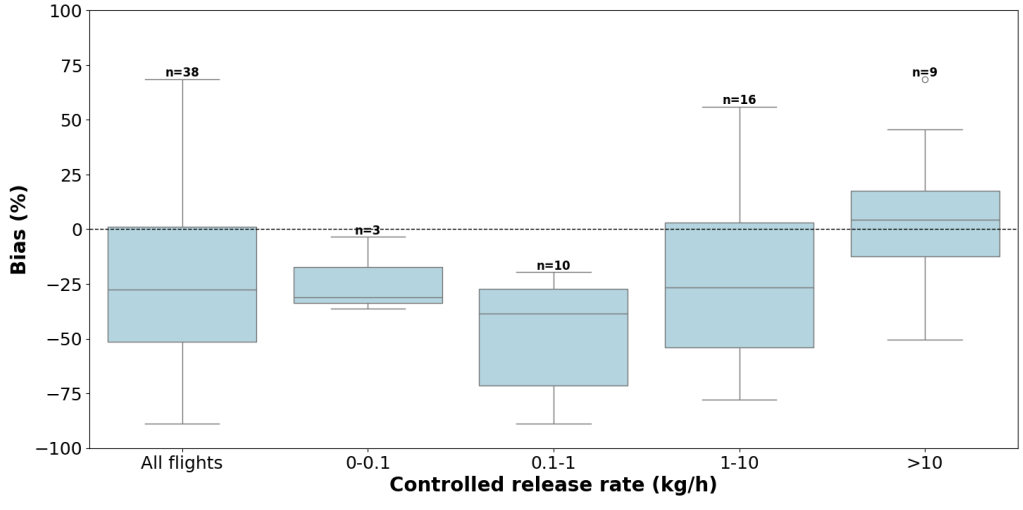


**Figure 5.** Box-and-whisker plots of the relative $CH_4$ flux bias (%) derived from UAV-based quantification flights at different controlled release rates during the NPL experiments. Each box represents the interquartile range (IQR) of the flight-level biases, with the central line showing the median and whiskers extending to 1.5×IQR. The "All flights" box on the left summarizes the bias distribution across all release rates. The numbers above each box indicate the number of individual flight measurements (n) included in each group.

https://doi.org/10.5194/egusphere-2026-1665
Preprint. Discussion started: 21 April 2026


**Table 3.** Percentage of flights where the known release rate lies within the uncertainty bounds of the estimated emission rates for each site.

| Site | Raw data | After adding extrapolated flux |
|---|---|---|
| Bedford | 41.6 | 70.8 |
| CEDAR | 50.0 | 71.4 |
| Combined | 46.1 | 71.7 |

Nevertheless, the underestimation of emissions by UAV-based techniques due to flight restrictions (for safety reasons or obstacles) is now a known and prescient challenge to the measurement community. Previous studies (e.g., McManemin et al., 2025) have already discussed the impacts of plume blowover i.e. methane escaping above or below the flight path. In their controlled release experiment there were four UAV participants and all of them found an underestimation of the released rate (slopes from 0.09 to 0.82). They attributed the discrepancy to the expected blowover and environmental conditions, with the principal factor being environmental wind speed and variability. Hamedani Raja et al. (2025) found that the main reason of the discrepancy is underestimation in the wind speed.

To reduce the low bias in the emission quantification, it is essential to fly the UAV as low as possible, or complement UAV-based measurements with additional surface measurements by ground-based techniques. In case this is not feasible due to safety constraints or because it is rather complicated and (cost and logistically) expensive, it is important to develop the measurement plane further away from the source, thus allowing sufficient mixing of the gas and reducing any near-surface impact due to dead sampling.

In order to deal with this underestimation issue, we extrapolated the measurements of the lowest transect to the ground level to fill the gap above the surface (Sect. 2.2.1). Table 3 shows the percentage of flights where the known release rate lies within the uncertainty bounds of the estimated emission rates for each site. Indeed, the agreement between the known and the estimated fluxes has increased after this modification, as the percentage increased from 41.6 to 70.8% and from 50 to 71.4% for Bedford and CEDAR, respectively. However, discrepancies still remain between the known and the estimated flux.

Figure 6 shows the flight-by-flight $CH_4$ fluxes derived from UAV measurements compared with known release rates. It is evident that UAVs can detect fine-scale $CH_4$ plumes down to 0.02 $\mathrm{kg\ h^{-1}}$, and flux trends are reliably captured (with methods and instruments similar in precision to those used in our study). The majority of the flights agree with the controlled release rates within calculated $1\sigma$ uncertainties, demonstrating robustness (Table 3). The largest bias of -60.5% is observed for flights 20–24 in Bedford (Fig. 6 a), all 5 flights in this rate (0.45 $\mathrm{kg\ h^{-1}}$) are conducted in 16/05/2024 when the average wind speed during the flights ranges from 2.3-3.2 $\mathrm{m\ s^{-1}}$, the lowest wind speed compared to the rest of the flights. Slack winds, in combination with the lower temperature of the released $CH_4$ compared to the ambient air might result in laminar flow and accumulation of the gas close to the ground and at the proximity of the release location, while the measurement plane is located approximately 100 m further way. Previous studies have also reported increased accuracy in the mass balance method when the winds are not weak and variable (Yang et al., 2018; Morales et al., 2022), thus it is recommended to avoid such conditions (Fosco et al., 2024).

https://doi.org/10.5194/egusphere-2026-1665
Preprint. Discussion started: 21 April 2026


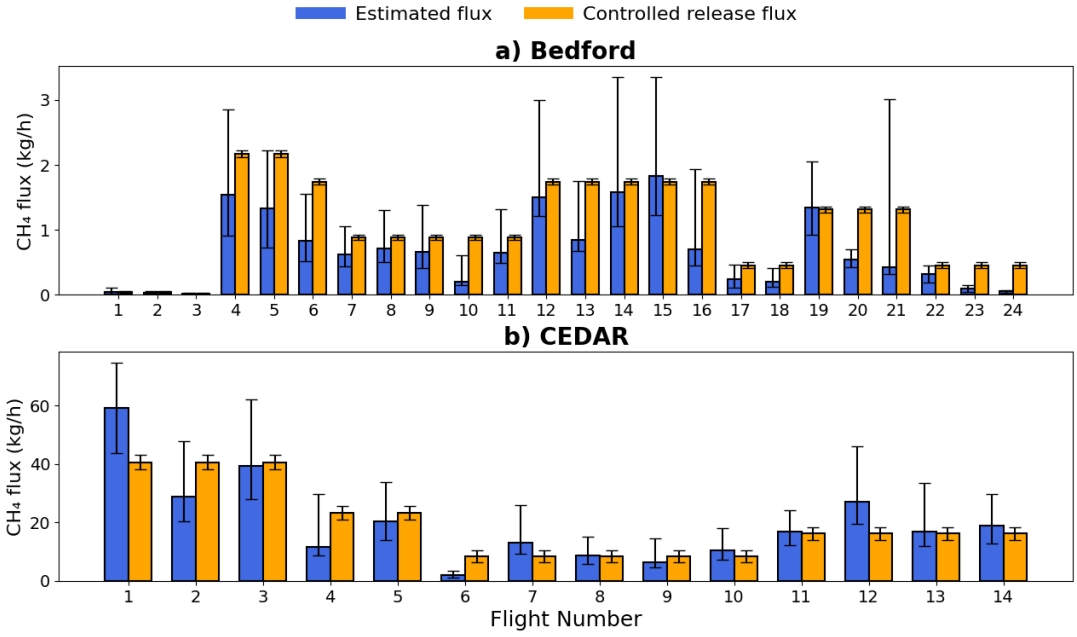


**Figure 6.** Flight-by-flight comparison of $CH_4$ fluxes derived from UAV-based measurements (blue) with the corresponding controlled release fluxes (orange). Error bars represent the uncertainty in each estimate; for UAV-derived fluxes, the positive error bar includes the extrapolated near-ground contribution. Results from the Bedford experiment are shown in panel (a), and those from the CEDAR experiment are shown in panel (b).

To identify potential factors that most strongly influence the quality of the agreement between the estimated and controlled release rates, Fig. 7 presents linear regression analyses between the absolute flux bias (%) and six explanatory parameters related to wind conditions, source geometry, and release characteristics: mean wind speed, standard deviation of wind direction, distance from the source, controlled release rate, $\Delta\theta$, and the percentage of measurements outside $\Delta\theta$. We define a source–transect angular window, $\Delta\theta$, as the angular range defined at the source by lines connecting the source to the endpoints of the UAV measurement transect. This window represents the range of wind directions for which emissions released at the source are advected towards and intersect the UAV sampling plane. To further assess the combined influence and relative importance of these factors, a correlation matrix is shown in Fig. 8. To increase the sample size and enable a more comprehensive analysis, data from Bedford and CEDAR are combined.

Both the linear regression and the correlation matrix results indicate that the mean wind speed is the dominant factor influencing the bias, with a correlation coefficient of -0.35. This negative correlation indicates that the absolute bias decreases with increasing wind speed, consistent with physical expectations and previous studies (e.g. Fosco et al., 2024; Yong et al., 2024)). Higher wind speeds promote more laminar plume advection and reduced turbulent dispersion, reducing near-surface stagnation effects and improving the likelihood that the plume is fully sampled by the measurement system. Based on the linear regression, the minimum wind speed required to achieve an absolute bias below 50% is approximately 2.21 $\mathrm{m\ s^{-1}}$, a threshold

https://doi.org/10.5194/egusphere-2026-1665
Preprint. Discussion started: 21 April 2026


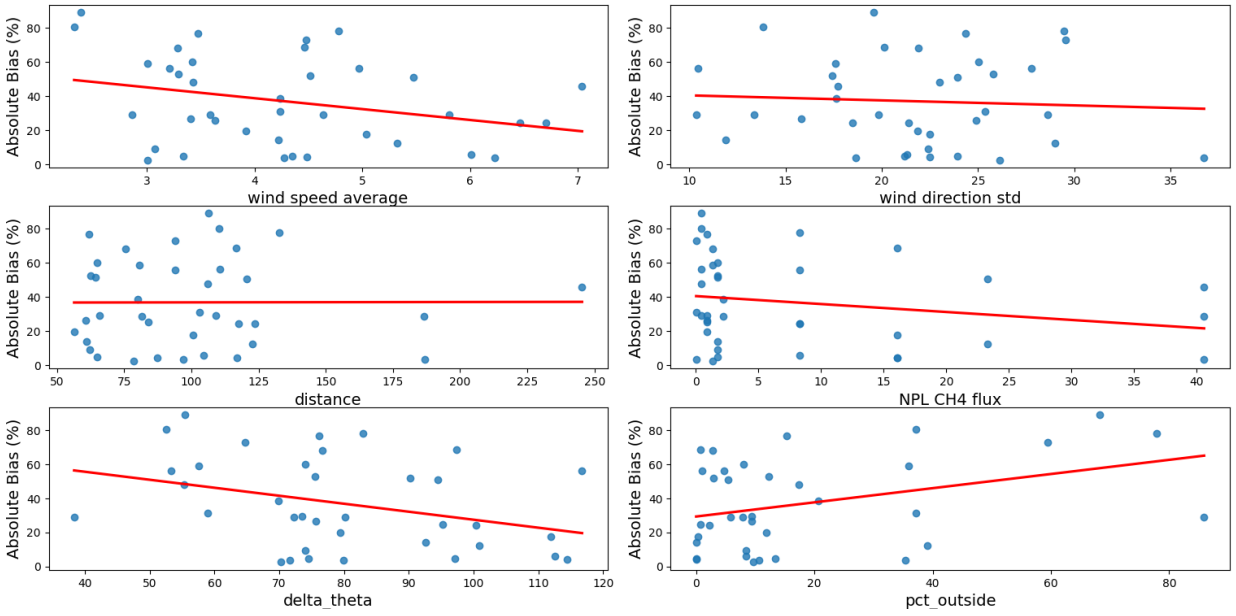


**Figure 7.** Absolute bias (%) as a function of six features: wind speed average, wind direction standard deviation, distance from the source, controlled release rate, $\Delta\theta$, and the percentage of measurements outside $\Delta\theta$. $\Delta\theta$ denotes the source–transect angular window (i.e. the range of wind directions for which the plume is expected to intersect the UAV measurement plane). Linear fit (red line) is shown in each subplot.

that is broadly consistent with wind speed criteria commonly reported in other studies for reliable flux quantification (e.g. Yang et al., 2018; Morales et al., 2022, 2.3 $\mathrm{m\ s^{-1}}$).

325 During the controlled release experiments, atmospheric conditions at both sites varied between neutral-buoyant and convective-buoyant. The mass balance method performed reliably under both stability regimes when sufficient horizontal wind was present (>2.21 $\mathrm{m\ s^{-1}}$). However, in low-wind conditions and under convective buoyancy, the plume transport was dominated by vertical turbulence rather than horizontal advection, and portions of the plume may not have crossed the downwind measurement plane. This behaviour aligns with the wind-speed threshold identified here and highlights why conditions of near-zero horizontal wind remain challenging for mass balance flux quantification.

Interestingly, the standard deviation of wind direction exhibits little direct correlation with absolute bias, suggesting that wind direction variability alone does not systematically degrade agreement. This does not imply that wind direction variability is unimportant; rather, it shows that the impact of such variability depends primarily on whether the lateral extent of sampling (as quantified by the source–transect angular window $\Delta\theta$) is capable of accommodating variations in plume location. In this 335 context, geometric factors describing the lateral extent of the measurement plane play a more critical role than the magnitude of directional variability itself.

Consistent with this interpretation, both $\Delta\theta$ and the percentage of measurements within $\Delta\theta$ emerge as important contributors to the agreement (correlations of -0.34 and +0.36, respectively). A larger lateral extent increases the probability that the

https://doi.org/10.5194/egusphere-2026-1665
Preprint. Discussion started: 21 April 2026


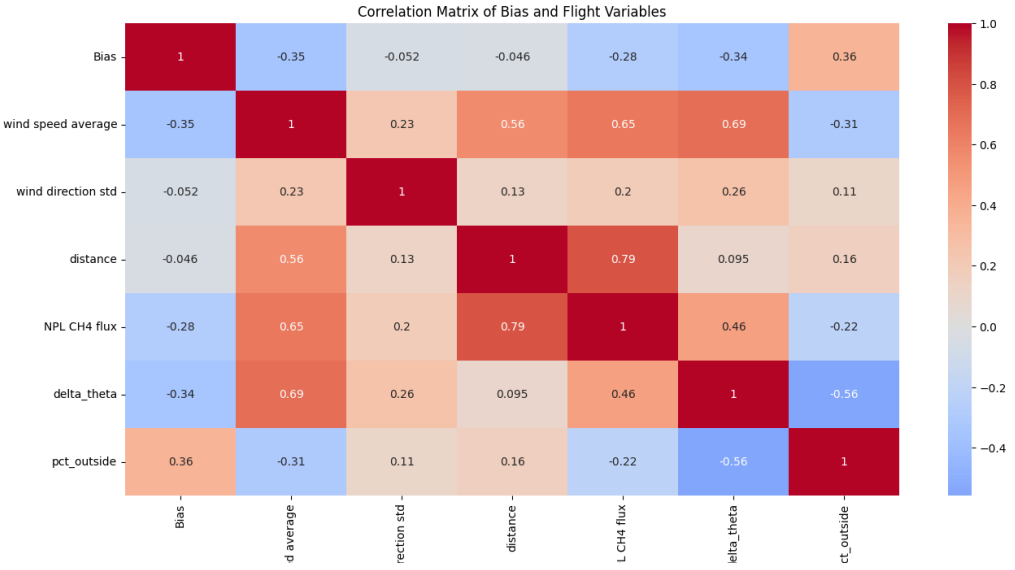


**Figure 8.** Correlation matrix of absolute bias (%) and six features: mean wind speed, standard deviation of wind direction, distance from the source, controlled release rate, $\Delta\theta$, and the percentage of measurements outside $\Delta\theta$.

plume remains within the sampled region (flux plane) under changing wind directions, thereby reducing plume sampling loss and associated under-bias. When the lateral extent of sampling is insufficient (i.e. not wide enough to capture all projections of the plume under variable wind conditions), even moderate fluctuations in wind direction can result in portions of the plume advecting outside the measurement plane, leading to increased absolute bias. These results highlight the importance of designing sampling configurations that are robust to potential wind direction variability by ensuring sufficiently wide lateral coverage. In other words, it is more important to sample more dead space (meaning a greater sampling time) than to miss a part of any plume (meaning poorer overall accuracy and bias).

In contrast, the distance between the controlled release point and the UAV measurement plane shows a negligible correlation with the absolute bias within the range of distances sampled in this study. This indicates that for the controlled-release experiments considered here, variations in downwind sampling distance do not systematically influence the agreement between estimated and known fluxes. This is expected for any mass-balance approach, as the integrated flux through the measurement plane should, in principle, be conserved with downwind distance, provided that the plume remains well captured within the sampling cross section.

Finally, the controlled release rate shows a moderate negative correlation with absolute bias (-0.28). As discussed previously, lower release rates mean that emissions quantified by mass balance are implicitly more sensitive to environmental variability, particularly wind fluctuations and background variability, and small absolute deviations can translate into large relative errors

https://doi.org/10.5194/egusphere-2026-1665
Preprint. Discussion started: 21 April 2026


when expressed as a percentage. At higher release rates, similar absolute deviations correspond to smaller relative biases, resulting in improved agreement.

## 4 Conclusions

In this study, we evaluate a UAV-based mass-balance approach for methane emission quantification using single-blind controlled-release experiments operated by the NPL at two UK sites: an isolated aerodrome in Bedford and an operational agricultural facility, CEDAR, with measurement transects positioned downwind of the controlled release to avoid interference from adjacent sources. Overall, methane releases spanned a wide range of emission rates (0.021-2.16 $\mathrm{kg\ h^{-1}}$ in Bedford and 8.3–40.6 $\mathrm{kg\ h^{-1}}$ in CEDAR) and included both point and extended source configurations representative of fugitive natural gas leaks, agricultural (manure) and landfill emission scenarios.

Two complementary validation approaches were applied: analysis of flux results from individual flights to capture operational variability, and grouping of flights by release rate to assess underlying method performance. Overall, fluxes calculated using the method show good correlation but substantial scatter at the individual flight level (CEDAR: slope = 1.01, $r$ = 0.84, RMSE = 38.8%; Bedford: slope = 0.71, $r$ = 0.85, RMSE = 46.2%) and improved agreement when averaged by release rate (CEDAR: slope = 1.01, $r$ = 0.94, RMSE = 19.9%; Bedford: slope = 0.68, $r$ = 0.99, RMSE = 38.4%). This indicates that averaging results from multiple flight surveys reduces random variability associated with environmental conditions while preserving systematic biases. The systematic underestimation observed here is consistent with previous UAV-based studies and is primarily attributable to flight constraints that limit sampling in the near-surface region.

Analysis of the linear regression and correlation matrix results provides further insight into the conditions under which the method performs most reliably. Mean wind speed emerges as the dominant environmental factor influencing agreement, with higher wind speeds associated with reduced absolute bias, and a minimum wind speed threshold of approximately 2.2 $\mathrm{m\ s^{-1}}$ required to achieve biases below 50%. This highlights the importance of conducting UAV-based mass-balance measurements under sufficiently strong wind conditions (we recommend 2-5 $\mathrm{m\ s^{-1}}$ for setups similar to those in this study) to ensure effective plume advection and sampling. By contrast, wind direction variability alone shows little direct influence on the bias; instead, the results demonstrate that the robustness of the measurement geometry to such variability is critical. In particular, wider lateral extent of the measurement plane significantly reduces plume loss under changing wind directions, underscoring the need for survey sampling strategies that are tolerant to realistic wind variability.

Within the range of experimental conditions investigated, the distance between the controlled release point and the UAV measurement plane does not systematically affect agreement, consistent with mass conservation expectations when the plume is adequately captured. The controlled release rate shows a moderate influence on relative bias, with lower emission rates exhibiting greater sensitivity to atmospheric variability and measurement uncertainty, resulting in larger percentage bias errors.

Differences in precision and bias between the two experimental sites further demonstrate the importance of experimental design and flight strategy. Improved agreement observed during the CEDAR experiment is attributed in part to the use of automated waypoint flight paths and sampling further downwind, which enabled repeatable and objective sampling with consistent

https://doi.org/10.5194/egusphere-2026-1665
Preprint. Discussion started: 21 April 2026


speed, altitude, and spatial coverage. Lower flight speeds increased plume sampling density and integration time, reducing measurement variability and minimising the potential for wind error from anemometers onboard. Together with generally higher release rates and stronger wind conditions, these factors contributed to improved performance relative to the manually flown Bedford experiment.

The improved performance observed after averaging is consistent with previous studies indicating that multiple flights per release rate (e.g. $n \geq 3$) enhance representativeness by reducing the influence of environmental variability. Overall, this study demonstrates that UAV-based mass-balance methods can provide accurate and robust methane emission estimates under controlled conditions, provided that measurements are conducted under suitable wind regimes and that survey sampling strategies are designed to ensure sufficient spatial sampling and complete plume interception. Typical flux uncertainty using the mass balance method described in this work can be summarised as 20% for emissions >10 $\mathrm{kg\ h^{-1}}$, worsening to ∼40% for emissions <2 $\mathrm{kg\ h^{-1}}$, based on RMSEs found for each site (and their respective emission range). In principle, this uncertainty could be improved further for future work (should greater precision be required) with repeated measurement surveys, so long as emissions can be expected to be static in time. These findings provide practical guidance for the planning of UAV deployments and the definition of data quality criteria for future applications targeting agricultural and landfill emission sources. To this end, we have included a digital attachment to the paper, which includes the Python source code used to calculate fluxes in this work in the hope that it can benefit others developing UAV mass balance approaches and build trust in emissions calculated using it by stakeholders such as regulators, industry and those involved in greenhouse gas inventory compilation and validation.

## Appendix A: Background $CH_4$ concentration for mass balance

To determine the background $CH_4$ concentration, we analysed the distribution of $CH_4$ measurements from each flight by constructing a histogram of all recorded data points (Fig. A1). The background concentration was identified as the mode of the distribution—the value with the highest frequency. Background measurements were obtained from the edges of the gas plume, as the flight path was extended toward the plume's outer limits.

https://doi.org/10.5194/egusphere-2026-1665
Preprint. Discussion started: 21 April 2026


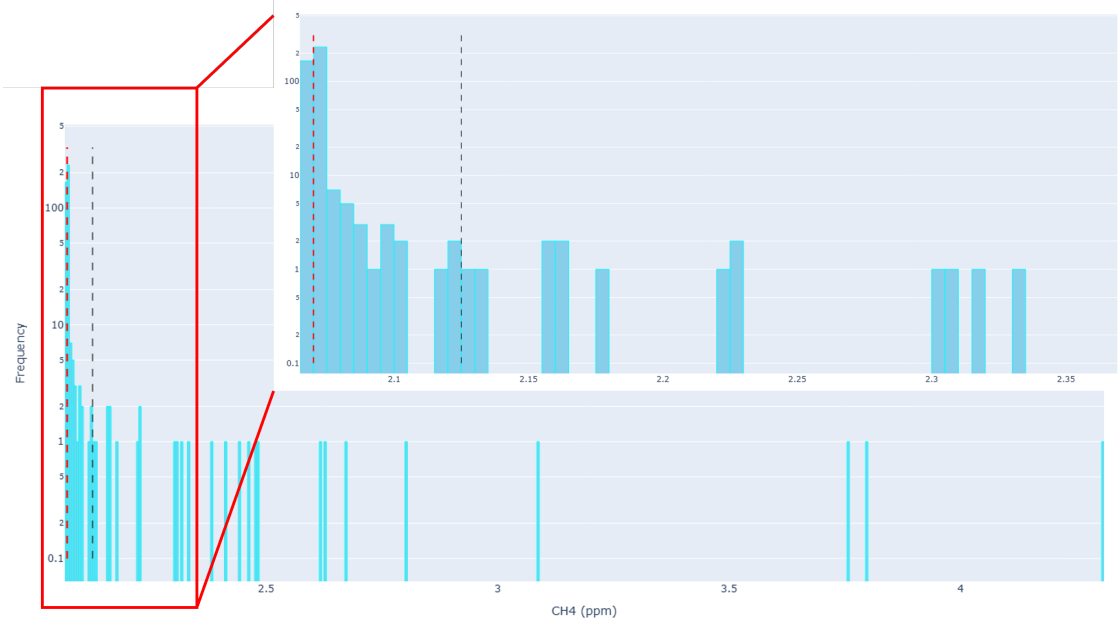


**Figure A1.** Histogram of $CH_4$ measurements from Flight 16 on 15 May 2024. The modal concentration (red dashed line; 2.070 ppm) was selected as the representative background $CH_4$ concentration. The uncertainty range (black dashed line; 2.125 ppm) corresponds to $\pm 1$ standard deviation, visually estimated around the mode, and was used to propagate uncertainty in the flux calculations (see Sect. 2.2).

https://doi.org/10.5194/egusphere-2026-1665
Preprint. Discussion started: 21 April 2026


One advantage of this approach is that it eliminates the need for upwind flights to estimate background concentrations, allowing for increased data collection within the plume itself (Yong et al., 2024). However, because both plume and background points are included within the same dataset, the resulting distribution is skewed, making it difficult to clearly separate background from plume measurements. To address this, we manually selected the background range by identifying the point where the left side of the distribution transitions into the tail. This range was selected to assess background variability, which allows for estimating the uncertainty in the background concentration and, consequently, the flux calculation (see Equation 1).

*Author contributions.* MT, JM, HR, KW, and GA collected the UAV-based data. JM led the initial development of the Python emissions quantification software which is publicly available in https://github.com/gasflux/gasflux/tree/develop. MT further developed this software, implemented the remaining analysis code, interpreted the results, and drafted the manuscript. GA provided scientific supervision and guidance throughout the analysis and manuscript preparation and contributed editorial revisions to the manuscript. JH led the controlled release experiments in collaboration with NPL and contributed to the description of the experimental setup. HR, KW and DL reviewed and commented on the manuscript.

*Competing interests.* The authors declare that they have no conflict of interest.

*Code and data availability.* The code used for emissions quantification in this study is publicly available. The initial development of the Python emissions quantification software was led by Jamie McQuilkin and is available at: https://github.com/gasflux/gasflux/tree/develop. The extended and updated quantification code used in this work is available at: https://github.com/mtsivlidou/controlled_release_exp.

The data supporting the findings of this study are available upon request and were made available to reviewers during the peer review process. The data will be made publicly available in an appropriate repository upon publication of the paper.

*Acknowledgements.* Firstly, we posthumously dedicate this article to our colleague and co-author, Jamie McQuilkin, who left us far too early in December 2025. We gratefully acknowledge Jamie McQuilkin for his contributions to this paper. Jamie McQuilkin collected UAV data in the Bedford controlled release campaign and led much of the initial development of the Python emissions quantification software provided along with this paper. Jamie was passionate that this software be provided openly to all, to build trust in emissions quantification methods.

We further acknowledge the strong support of the National Physical Laboratory for providing controlled release facilities and technical support. We also acknowledge Aimee Buck and Zuhaib Khan of the National Physical Laboratory for their significant contributions: Aimee led the operation of the controlled release facilities at both Bedford and CEDAR, and Zuhaib processed the data from these campaigns.

AI tools (such as ChatGPT) were used for light language editing of this manuscript and code assistance.

This work was supported by the UK's Natural Environment Research Council (NERC) [grant number NE/X014649/1] under the MOMENTUM project.

https://doi.org/10.5194/egusphere-2026-1665
Preprint. Discussion started: 21 April 2026


## References

Allen, G., Gallagher, M., Hollingsworth, P., Illingworth, S., Kabbabe, K., and Percival, C.: Feasibility of aerial measurements of methane emissions from landfills, Tech. Rep. SC130034/R, Environment Agency, Bristol, UK, 2014.

Allen, G., Pitt, J., Hollingsworth, P., Mead, I., Kabbabe, K., Roberts, G., and Percival, C.: Measuring landfill methane emissions using unmanned aerial systems: field trial and operational guidance, Tech. rep., Environment Agency, 2015.

Allen, G., Williams, P., Ricketts, H., Shah, A., Hollingsworth, P., Kabbabe, K., Helmore, J., Finlayson, A., Robinson, R., Rees-White, T., Beaven, R., Scheutz, C., and Fredenslund, A. M.: Validation of landfill methane measurements from an unmanned aerial system: Project SC 160006, Tech. rep., Environment Agency, UK, https://www.gov.uk/government/publications/validation-of-landfill-methane-measurements-from-an-unmanned-aerial-system, 2018.

Allen, G., Hollingsworth, P., Kabbabe, K., Pitt, J. R., Mead, M. I., Illingworth, S., Roberts, G., Bourn, M., Shallcross, D. E., and Percival, C. J.: The development and trial of an unmanned aerial system for the measurement of methane flux from landfill and greenhouse gas emission hotspots, Waste Management, 87, 883–892, https://doi.org/10.1016/j.wasman.2019.03.044, 2019.

Barker, P. A., Allen, G., Pitt, J. R., Bauguitte, S. J.-B., Pasternak, D., Cliff, S., France, J. L., Fisher, R. E., Lee, J. D., Bower, K. N., et al.: Airborne quantification of net methane and carbon dioxide fluxes from European Arctic wetlands in Summer 2019, Philosophical Transactions of the Royal Society A, 380, 20210 192, 2022.

Bonne, J.-L., Donnat, L., Albora, G., Burgalat, J., Chauvin, N., Combaz, D., Cousin, J., Decarpenterie, T., Duclaux, O., Dumelié, N., et al.: A measurement system for CO 2 and CH 4 emissions quantification of industrial sites using a new in situ concentration sensor operated on board uncrewed aircraft vehicles, Atmospheric Measurement Techniques, 17, 4471–4491, 2024.

Connor, A., Shaw, J. T., Yarrow, N., Howes, N., Helmore, J., Finlayson, A., Barker, P., and Robinson, R.: A framework for describing and classifying methane reporting requirements, emission sources, and monitoring methods, Environmental Science: Atmospheres, 4, 1203–1217, 2024.

Cooper, J., Dubey, L., and Hawkes, A.: Methane detection and quantification in the upstream oil and gas sector: the role of satellites in emissions detection, reconciling and reporting, Environmental Science: Atmospheres, 2, 9–23, https://doi.org/10.1039/D1EA00046B, 2022.

DJI: Matrice 600 Pro, https://www.dji.com/uk, last access: 13 March 2025, 2025.

Etminan, M., Myhre, G., Highwood, E. J., and Shine, K. P.: Radiative forcing of carbon dioxide, methane, and nitrous oxide: A significant revision of the methane radiative forcing, Geophysical Research Letters, 43, 12 614–12 623, https://doi.org/10.1002/2016GL071930, 2016.

Feitz, A., Schroder, I., Phillips, F., Coates, T., Neghandhi, K., Day, S., Luhar, A., Bhatia, S., Edwards, G., Hrabar, S., Hernandez, E., Wood, B., Naylor, T., Kennedy, M., Hamilton, M., Hatch, M., Malos, J., Kochanek, M., Reid, P., Wilson, J., Deutscher, N., Zegelin, S., Vincent, R., White, S., Ong, C., George, S., Maas, P., Towner, S., Wokker, N., and Griffith, D.: The Ginninderra $CH_4$ and $CO_2$ release experiment: An evaluation of gas detection and quantification techniques, International Journal of Greenhouse Gas Control, 70, 202–224, https://doi.org/10.1016/j.ijggc.2017.11.018, 2018.

Fosco, D., De Molfetta, M., Renzulli, P., and Notarnicola, B.: Progress in monitoring methane emissions from landfills using drones: an overview of the last ten years, Science of the Total Environment, 945, 173 981, https://doi.org/10.1016/j.scitotenv.2024.173981, 2024.

Global Methane Pledge: Global Methane Pledge website: Pledges, https://globalmethanepledge.ccacoalition.org/#pledges, last access: 22 September 2025, 1 September, 2023.

https://doi.org/10.5194/egusphere-2026-1665
Preprint. Discussion started: 21 April 2026


Hamedani Raja, S., Bullock, T., Laurikainen, M., and Irjala, M.: Assessing anomalies in methane mass flow estimation: Investigating findings and lessons for enhanced monitoring, https://doi.org/10.5281/zenodo.14882794, zenodo preprint, 2025.

IPCC: Climate Change 2023: Synthesis Report, Summary for Policymakers. Contribution of Working Groups I, II and III to the Sixth Assessment Report of the Intergovernmental Panel on Climate Change, Tech. rep., Intergovernmental Panel on Climate Change, Geneva, Switzerland, https://doi.org/10.59327/IPCC/AR6-9789291691647, 2023.

Jacob, D. J., Varon, D. J., Cusworth, D. H., Dennison, P. E., Frankenberg, C., Gautam, R., Guanter, L., Kelley, J., McKeever, J., Ott, L. E., Poulter, B., Qu, Z., Thorpe, A. K., Worden, J. R., and Duren, R. M.: Quantifying methane emissions from the global scale down to point sources using satellite observations of atmospheric methane, Atmospheric Chemistry and Physics Discussions, pp. 1–44, https://doi.org/10.5194/acp-2022-94, 2022.

Lamb, B. K., Edburg, S. L., Ferrara, T. W., Howard, T., Harrison, M. R., Kolb, C. E., Townsend-Small, A., Dyck, W., Possolo, A., and Whetstone, J. R.: Direct Measurements Show Decreasing Methane Emissions from Natural Gas Local Distribution Systems in the United States, Environmental Science & Technology, 49, 5161–5169, https://doi.org/10.1021/es505116p, 2015.

Li, Y., Zhang, C., Su, W., Jiang, S., Nie, D., Wang, Y., Wang, Y., He, H., Chen, Q., Martin, S. T., and Ye, J.: Copter-Type UAV-Based Sensing in Atmospheric Chemistry: Recent Advances, Applications, and Future Perspectives, Environmental Science & Technology, https://doi.org/10.1021/acs.est.5c00074, 2025.

Liu, Y., Paris, J.-D., Broquet, G., Bescós Roy, V., Meixus Fernandez, T., Andersen, R., Russu Berlanga, A., Christensen, E., Courtois, Y., Dominok, S., et al.: Assessment of current methane emissions quantification techniques for natural gas midstream applications, Atmospheric Measurement Techniques Discussions, 2023, 1–27, 2023.

Mays, K. L., Shepson, P. B., Stirm, B. H., Karion, A., Sweeney, C., and Gurney, K. R.: Aircraft-based measurements of the carbon footprint of Indianapolis, Environmental Science & Technology, 43, 7816–7823, 2009.

McManemin, A., Juéry, C., Blandin, V., France, J. L., Burdeau, P., and Brandt, A. R.: Controlled release testing of commercially available methane emission measurement technologies at the TADI facility, EGUsphere, 2025, 1–21, 2025.

Mønster, J., Kjeldsen, P., and Scheutz, C.: Methodologies for measuring fugitive methane emissions from landfills—A review, Waste Management, 87, 835–859, https://doi.org/10.1016/j.wasman.2018.12.047, 2019.

Morales, R., Ravelid, J., Vinkovic, K., Korbeń, P., Tuzson, B., Emmenegger, L., Chen, H., Schmidt, M., Humbel, S., and Brunner, D.: Controlled-release experiment to investigate uncertainties in UAV-based emission quantification for methane point sources, Atmospheric Measurement Techniques, 15, 2177–2198, https://doi.org/10.5194/amt-15-2177-2022, 2022.

Myers, D. E.: Interpolation and estimation with spatially located data, Chemometrics and Intelligent Laboratory Systems, 11, 209–228, 1991.

Pandey, S., Houweling, S., Lorente, A., Borsdorff, T., Tsivlidou, M., Bloom, A. A., Poulter, B., Zhang, Z., and Aben, I.: Using satellite data to identify the methane emission controls of South Sudan's wetlands, Biogeosciences, 18, 557–572, https://doi.org/10.5194/bg-18-557-2021, 2021.

Pitt, J. R., Allen, G., Bauguitte, S. J.-B., Gallagher, M. W., Lee, J. D., Drysdale, W., Nelson, B., Manning, A. J., and Palmer, P. I.: Assessing London $CO_2$, $CH_4$ and CO emissions using aircraft measurements and dispersion modelling, Atmospheric Chemistry and Physics, 19, 8931–8945, https://doi.org/10.5194/acp-19-8931-2019, 2019.

Prather, M. J., Holmes, C. D., and Hsu, J.: Reactive greenhouse gas scenarios: Systematic exploration of uncertainties and the role of atmospheric chemistry, Geophysical Research Letters, 39, L09 803, https://doi.org/10.1029/2012GL051440, 2012.

Riddick, S. N., Mbua, M., Riddick, J. C., Houlihan, C., Hodshire, A. L., and Zimmerle, D. J.: Uncertainty quantification of methods used to measure methane emissions of 1 g CH4 h- 1, Sensors, 23, 9246, 2023.

https://doi.org/10.5194/egusphere-2026-1665
Preprint. Discussion started: 21 April 2026


Saunois, M., Martinez, A., Poulter, B., Zhang, Z., Raymond, P. A., Regnier, P., Canadell, J. G., Jackson, R. B., Patra, P. K., Bousquet, P., Ciais, P., Dlugokencky, E. J., Lan, X., Allen, G. H., Bastviken, D., Beerling, D. J., Belikov, D. A., Blake, D. R., Castaldi, S., Crippa, M., Deemer, B. R., Dennison, F., Etiope, G., Gedney, N., Höglund-Isaksson, L., Holgerson, M. A., Hopcroft, P. O., Hugelius, G., Ito, A., Jain, A. K., Janardanan, R., Johnson, M. S., Kleinen, T., Krummel, P. B., Lauerwald, R., Li, T., Liu, X., McDonald, K. C., Melton, J. R., Mühle, J., Müller, J., Murguia-Flores, F., Niwa, Y., Noce, S., Pan, S., Parker, R. J., Peng, C., Ramonet, M., Riley, W. J., Rocher-Ros, G., Rosentreter, J. A., Sasakawa, M., Segers, A., Smith, S. J., Stanley, E. H., Thanwerdas, J., Tian, H., Tsuruta, A., Tubiello, F. N., Weber, T. S., van der Werf, G. R., Worthy, D. E. J., Xi, Y., Yoshida, Y., Zhang, W., Zheng, B., Zhu, Q., Zhu, Q., and Zhuang, Q.: Global Methane Budget 2000–2020, Earth System Science Data, 17, 1873–1958, https://doi.org/10.5194/essd-17-1873-2025, 2025.

Scheutz, C., Knudsen, J. E., Vechi, N. T., and Knudsen, J.: Validation and demonstration of a drone-based method for quantifying fugitive methane emissions, Journal of Environmental Management, 373, 123 467, https://doi.org/10.1016/j.jenvman.2024.123467, 2025.

Schuit, B. J., Maasakkers, J. D., Bijl, P., Mahapatra, G., van den Berg, A.-W., Pandey, S., Lorente, A., Borsdorff, T., Houweling, S., Varon, D. J., McKeever, J., Jervis, D., Girard, M., Irakulis-Loitxate, I., Gorroño, J., Guanter, L., Cusworth, D. H., and Aben, I.: Automated detection and monitoring of methane super-emitters using satellite data, Atmospheric Chemistry and Physics, 23, 9071–9098, https://doi.org/10.5194/acp-23-9071-2023, 2023.

Shah, A., Pitt, J. R., Ricketts, H., Brian Leen, J., Williams, P. I., Kabbabe, K., Gallagher, M. W., and Allen, G.: Testing the near-field Gaussian plume inversion flux quantification technique using unmanned aerial vehicle sampling, Atmospheric Measurement Techniques, 13, 1467–1484, https://doi.org/10.5194/amt-13-1467-2020, 2020a.

Shah, A., Ricketts, H., Pitt, J. R., Shaw, J. T., Kabbabe, K., Leen, J. B., and Allen, G.: Unmanned aerial vehicle observations of cold venting from exploratory hydraulic fracturing in the United Kingdom, Environmental Research Communications, 2, 021 003, 2020b.

Shan, Y., Tian, K., Li, R., Guan, Y., Ou, J., Guan, D., and Hubacek, K.: Global methane footprints growth and drivers 1990–2023, Nature Communications, 16, 8184, https://doi.org/10.1038/s41467-025-63383-5, 2025.

Shaw, J. T., Shah, A., Yong, H., and Allen, G.: Methods for quantifying methane emissions using unmanned aerial vehicles: a review, Philosophical Transactions of the Royal Society A: Mathematical, Physical and Engineering Sciences, 379, 20200 450, https://doi.org/10.1098/rsta.2020.0450, 2021.

Shindell, D., Kuylenstierna, J. C. I., Vignati, E., van Dingenen, R., Amann, M., Klimont, Z., Anenberg, S. C., Muller, N., Janssens-Maenhout, G., Raes, F., Schwartz, J., Faluvegi, G., Pozzoli, L., Kupiainen, K., Höglund-Isaksson, L., Emberson, L., Streets, D., Ramanathan, V., Hicks, K., Oanh, N. T. K., Milly, G., Williams, M., Demkine, V., and Fowler, D.: Simultaneously Mitigating Near-Term Climate Change and Improving Human Health and Food Security, Science, 335, 183–189, https://doi.org/10.1126/science.1210026, 2012.

Souza, W. S. R., Hart, A. J., Fonseca, B. J. B., Tahernezhadi, M., and Christensen, L. E.: A framework to survey a region for gas leaks using an unmanned aerial vehicle, IEEE Access, 12, 1386–1407, https://doi.org/10.1109/ACCESS.2023.3345801, 2024.

SPH Engineering: UgCS Flight Planning, https://www.sphengineering.com/flight-planning, last access: 13 March 2025, 2025.

Tettenborn, J., Zavala-Araiza, D., Stroeken, D., Maazallahi, H., van der Veen, C., Hensen, A., Velzeboer, I., van den Bulk, P., Vogel, F., Gillespie, L., et al.: Improving consistency in methane emission quantification from the natural gas distribution system across measurement devices, EGUsphere, 2025, 1–27, 2025.

Tibrewal, K., Ciais, P., Saunois, M., Martinez, A., Lin, X., Thanwerdas, J., Deng, Z., Chevallier, F., Giron, C., Albergel, C., Tanaka, K., Patra, P., Tsuruta, A., Zheng, B., Belikov, D., Niwa, Y., Janardanan, R., Maksyutov, S., Segers, A., Tzompa-Sosa, Z. A., Bousquet, P., and Sciare, J.: Assessment of methane emissions from oil, gas and coal sectors across inventories and atmospheric inversions, Communications Earth & Environment, 5, 26, https://doi.org/10.1038/s43247-023-01190-w, 2024.

https://doi.org/10.5194/egusphere-2026-1665
Preprint. Discussion started: 21 April 2026


Tong, X., van Heuven, S., Scheeren, B., Kers, B., Hutjes, R., and Chen, H.: Aircraft-Based AirCore sampling for estimates of $N_2O$ and $CH_4$ emissions, Environmental Science & Technology, 57, 15 571–15 579, https://doi.org/10.1021/acs.est.3c04244, 2023.

UNEP: Global Methane Assessment: Benefits and Costs of Mitigating Methane Emissions, Tech. rep., United Nations Environment Programme and Climate and Clean Air Coalition, Nairobi, ISBN 978-92-807-3854-4, 2021.

Vollrath, C., Hugenholtz, C. H., and Barchyn, T. E.: Onshore methane emissions measurements from the oil and gas industry: a scoping review, Environmental Research Communications, 6, 032 001, https://doi.org/10.1088/2515-7620/ad3129, 2024.

WMO: WMO Greenhouse Gas Bulletin No. 21: The State of Greenhouse Gases in the Atmosphere Based on Global Observations through 2024, WMO Greenhouse Gas Bulletin 21, World Meteorological Organization, https://wmo.int/sites/default/files/2025-10/GHG-21_en.pdf, 2025.

Yang, S., Talbot, R. W., Frish, M. B., Golston, L. M., Aubut, N. F., Zondlo, M. A., Gretencord, C., and McSpiritt, J.: Natural gas fugitive leak detection using an unmanned aerial vehicle: Measurement system description and mass balance approach, Atmosphere, 9, 383, https://doi.org/10.3390/atmos9100383, 2018.

Yong, H., Allen, G., Mcquilkin, J., Ricketts, H., and Shaw, J. T.: Lessons learned from a UAV survey and methane emissions calculation at a UK landfill, Waste Management, 180, 47–54, https://doi.org/10.1016/j.wasman.2024.03.025, 2024.